Title
Predictive Model for Hurricane Wind Hazard under Changing Climate Conditions

Journal
Natural Hazards Review, 22(3)

ISSN
1527-6988

Authors
Esmaeili, Mirsardar
Barbato, Michele

Publication Date
2021-08-01

DOI
10.1061/(asce)nh.1527-6996.0000458

Peer reviewed

Esmaeili M, Barbato M (2021). A predictive model for hurricane wind hazard under changing climate conditions. Natural Hazards Review (ASCE), 22(3): 04021011.
https://doi.org/10.1061/%28ASCE%29NH.1527-6996.0000458

A predictive model for hurricane wind hazard under changing climate conditions

Mirsardar Esmaeili[1], S.M.ASCE; and Michele Barbato[2], M.ASCE.

ABSTRACT

Hurricanes are among the most destructive and costliest extreme weather events. The intensity of future hurricanes is generally expected to increase due to climate change effects. In this work, a simulation method based on a comprehensive statistical analysis of historical data is developed to account for the changes in climatological conditions and their effects on the frequency and intensity of hurricanes. This method is applied to simulate the hurricane wind speed distributions under different climatological conditions in the US Atlantic Basin from Texas to Maine, which is one of the most vulnerable regions of the world to hurricane hazards. To this end, regression models for several different hurricane parameters are fit to the historical hurricane data. The proposed model is validated by comparing its predicted hurricane-induced wind speeds with available historical data and other existing models based on physics-based hurricane path simulation. This new model is found to reproduce very well historical wind speed distributions, and to provide wind speed projection results that are consistent with those of more computationally expensive models based on the simulation of hurricane tracks. The statistical characteristics of future potential hurricanes are simulated using the proposed model along with the climate projections presented in the 5th Assessment Report of the Intergovernmental Panel for Climate Change. The results of this study indicate that, by year 2060 and depending on the considered projection scenario, the design wind speeds along the US Gulf and Atlantic Coast corresponding to the different mean return intervals considered by ASCE 7 are expected to increase in average between 14% and 26%, which correspond to an average increase of the design wind-induced loads contained between 30% and 59%.

Keywords: Climate change; hurricanes; hurricane hazard; sea surface temperature; wind speed.

[1] Ph.D. student, Department of Civil & Environmental Engineering, University of California Davis, One Shields Avenue, 2209 Academic Surge, Davis, California 95616, USA; E-mail: mesmaeili@ucdavis.edu

[2] Professor, Department of Civil & Environmental Engineering, University of California Davis, One Shields Avenue, 3149 Ghausi Hall, Davis, California 95616, USA; E-mail: mbarbato@ucdavis.edu

Introduction

Tropical cyclones are extreme weather events that often cause extensive social and economic losses worldwide (Huang et al. 2001). The US Gulf and Atlantic Coast regions are frequently struck by these natural events, which are locally referred to as hurricanes. The growing number of resident population (Crossett et al. 2013) and the concentration of US energy production (Adams et al. 2004) contribute to increasing the hurricane vulnerability of this region. This fact is reflected by the massive losses (normalized to 2017 US dollar) caused by recent hurricanes, e.g., \$160 billion losses by Hurricane Katrina in 2005, \$125 billion losses by Hurricane Harvey in 2017, and \$50 billion losses by Hurricane Irma in 2017 (National Hurricane Center 2018). The observed trend based on 1900-2005 data indicates that hurricane losses in the US Gulf Coast region are doubling every 10 years (Pielke et al. 2008).

The phenomena commonly known as climate change are responsible for changes in the sea water level, sea water temperature, and intensity of extreme weather events, including hurricanes (Stocker et al. 2013). The current consensus among climate scientists is that climate change will very likely produce an intensification of future hurricanes, resulting in potential increases of hurricane-induced losses (Bjarnadottir et al. 2014; Elsner et al. 2011; Hallegatte 2007). By analyzing the data from high-resolution dynamic models, Knutson et al. (2010) concluded that the intensity of hurricanes will increase between 2-11% by 2100 due to global warming. Grinsted et al. (2013) observed that the most extreme weather events are very sensitive to changes in temperature and estimated that the frequency of Katrina-like events could double due to the global warming produced during the 20th century. Significant research has been devoted to modeling the intensification of hurricanes due to climate change (Bjarnadottir et al. 2011, 2014; Emanuel 2011; Knutson et al. 2007, 2013; Manuel et al. 2008), often based on the climate projection scenarios proposed by the Intergovernmental Panel on Climate Change (IPCC) (Stocker et al. 2013). Some studies approached the problem of estimating future hurricane intensities and corresponding expected induced losses from a statistical point of view based on the abundant available data (Elsner et al. 2011; Jagger et al. 2001; Malmstadt et al. 2010). More recently, hurricane path simulation has been used to predict future hurricane damages to structures and infrastructure systems in a warmer climate. Mudd et al. (2014) developed a framework for assessing climate change effects on the US East Coast hurricane hazards by modeling hurricane paths and decay by combining the Georgiou's hurricane wind speed model (Georgiou et al. 1983), an empirical hurricane track model (Vickery et al. 2000), and a hurricane genesis model depending on the sea surface temperature (SST) changes predicted by different climate scenarios (Stocker et al. 2013). Considering the worst-case climate change scenario, they found that the design wind speeds given by ASCE 7-10 for the US Northeast region should be increased by up to 15m/s for structures of risk category I and II, and up to 30m/s for structures of risk category III and IV to ensure that structures designed today will achieve appropriate target safety and expected performance levels in year 2100 (Mudd et al. 2014). Cui and Caracoglia (2016) developed a framework for estimating lifetime costs of tall buildings subject to hurricane-induced damages under different climate change scenarios by means of a statistical hurricane track path model. Under the worst-case scenario, they estimated that the hurricane-induced losses on tall buildings could increase up to 30% from 2015 to 2115. Lee and Ellingwood (2017) developed a framework for risk assessment of infrastructures with long expected service periods accounting for the effects of climate change by adopting the model by Vickery et al. (2000). Pant and Cha (2018) developed a framework to account for the effects of climate change on hurricane wind-induced damage and losses for residential buildings in the Miami-Dade County, FL. They used Georgiou's model (Georgiou et al. 1983) in conjunction with a transition matrix to simulate the hurricane track, and developed relationships between average yearly SST and hurricane parameters used for hurricane genesis. They found that, for each 1°C increase, the 3-second averaged wind speed for 700 years return period is expected to increase by about 6.7-8.9 m/s for the county, and the accumulated hurricane-induced losses in 2016 to 2055 period are expected to increase by 1.4 to 1.7 times the expected losses predicted for the 2006 climatological conditions.

Climate change affects all hazards associated with hurricane events, i.e., wind, windborne debris, storm surge, and rain hazards (Barbato et al. 2013; Unnikrishnan and Barbato 2017). This paper focuses only on hurricane wind hazard. The objective is to develop an accurate and efficient statistical model for wind hazard in coastal areas, which can account for the non-stationary climatological conditions produced by climate change. A simulation procedure based on the indirect statistics approach is proposed in this study.

This paper is organized as follows: (1) the vector of parameters necessary to describe the hurricane wind hazard, referred to as intensity measure (IM) vector, is identified and a statistical model is developed for its components as functions of climatological conditions, synthetically described by SST; (2) using a multi-layer Monte Carlo simulation approach and an existing hurricane wind profile model, a wind distribution simulation procedure for coastal sites and given SST is developed; (3) the model simulation capabilities are validated through a comparison with historical data from the National Institute of Standards and Technology (NIST 2016) and the design wind speeds from ASCE 7-16 (ASCE 2016); and (4) the results of the developed simulation approach are compared with those of other existing models based on simulation of hurricane tracks, i.e., the models developed by Cui and Caracoglia (2016) and Pant and Cha (2019), and the proposed models is used to develop hurricane wind speed distributions along the US Gulf and Atlantic Coast based on the climate scenarios presented in the IPCC 5th Assessment Report (AR5) (Stocker et al. 2013).

Research significance

This research proposes a predictive simulation approach to quantify the non-stationary effects of climate change on hurricane wind speeds along the US Gulf and Atlantic Coast. This simulation procedure innovatively uses a simple and efficient indirect statistics approach (Unnikrishnan and Barbato 2017), in which the statistics of the different IMs are indirectly obtained from site-specific statistics of fundamental hurricane parameters. The major contribution of this method is the lower computational cost when compared to full track approaches existing in the literature (Cui and Caracoglia 2016; Lee and Ellingwood 2017; Mudd et al. 2014; Pant and Cha 2018, 2019), which can allow researchers and practicing engineers to consider a significantly higher number of scenarios at only a fraction of the computational cost of a single scenario for a full track approach. The proposed methodology is specialized in this paper for the US Gulf and Atlantic Coast; however, it can be easily extended to other regions worldwide, by using appropriate statistical data from pertinent historical records.

Modeling of IMs as functions of SST

This study uses the SST at the location and time of a given hurricane, T, as the main indicator of climate change effects on hurricane properties. This selection is consistent with the high correlation between hurricane intensity and SST (Bjarnadottir et al. 2011; Elsner et al. 2012; Emanuel 2011, 1999; Vickery et al. 2000, 2009; Webster et al. 2005), explained by the increase in warm water evaporation that fuels hurricanes as SST increases. Consistently with an indirect statistics approach, the following subset of IM components were selected as the primary IMs affected by climate change: hurricane annual frequency, ν_{h}; peak hurricane wind speed (here defined as the maximum 1-minute average speed measured at 10 m height over open terrain), $V_{\max}$; radius to maximum wind speed, $R_{\max}$; and translational wind speed, V_{t} . These IM components were selected because they are consistent with the hurricane radial wind profile model proposed by Willoughby et al. (2006) to describe the pressure gradient component, $V_{\mathrm{r}}(r)$, of the hurricane wind speed at a given distance, r , from the hurricane eye.

All IMs except ν_{h} are modeled as functions of T to account for the non-stationary climatic conditions produced by climate change. In particular, means and standard deviations are defined by a linear regression model, the parameters of which are based on historical data, as follows:

$$\mu_p(T) = a_{p0} + a_{p1} \cdot T \tag{1}$$

$$\sigma_p(T) = b_{p0} + b_{p1} \cdot T \tag{2}$$

in which $p = V_{\max}, R_{\max}, V_{\mathrm{t}}$. For each IM, a modified Kolmogorov-Smirnov statistical test (Soong 2004) was used to identify an appropriate probability distribution. Note that this approach is different from that adopted in Pant and Cha (2018), in which the linear regression models of the hurricane parameters were developed as function of the average yearly SST, T_y.

Hurricane frequency model

Existing literature indicates a significant level of disagreement among different researchers regarding the variation in hurricane frequency and the development of an appropriate hurricane frequency model under changing climate conditions (Lombardo and Ayyub 2015). In this work, climate change-induced modifications of the hurricane annual frequency were investigated by analyzing the yearly number of hurricanes in the US Gulf and Atlantic Coast during the 1851-2018 period as a function of the yearly global T_y, which is plotted in Fig. 1(a) based on the hurricane records in the HURDAT2 database (Landsea et al. 2015). The slope of the linear regression model used to fit the historical data is almost equal to zero, i.e., the annual frequency for Atlantic hurricanes is independent of T_y (p-value = 0.95). The same methodology was followed to investigate the climate change effects on the hurricane annual frequency at different marine mileposts at intervals of 185.2 km (100 nautical miles) along the US Gulf and Atlantic Coast regions (shown in Fig. 1(b)), based on the hurricane annual frequencies given in the NIST database (NIST 2016). For all considered mileposts, the slope of the linear regression was found to be statistically equal to zero, with p-values ranging between 0.74 and 0.86. Based on the existing literature, two distributions were considered to model the hurricane annual occurrences: the Poisson distribution (Batts et al. 1980, Mudd et al. 2014) and the negative binomial distribution (Cui and Caracoglia 2016, Jagger and Elsner 2012, Oxenyuk et al. 2017, Vickery et al. 2000). A chi-squared goodness-of-fit test (Soong 2004) failed to reject the null hypothesis at a 5% significance level in 24 out of 27 locations for the Poisson distribution (i.e., the fitting of the available data with a Poisson distribution was acceptable for 24 out of 27 locations), and in 10 out of 27 locations for the negative binomial distribution (i.e., the fitting of the available data with a negative binomial distribution was acceptable for 10 out of 27 locations). It was also observed that, for the 17 locations where the negative binomial distribution was rejected, the sample mean of the number of hurricane annual occurrences was higher than the corresponding sample variance, confirming that the use of a negative binomial distribution was not appropriate for those locations.

Based on these results, the yearly number of hurricanes affecting a given location is modeled as a Poisson random variable with constant (i.e., not dependent on T_y) annual frequency, ν_{h}, equal at each location to the annual hurricane frequency given in the NIST database (NIST 2016). The values of ν_{h} corresponding to the considered mileposts along the US Gulf and Atlantic Coast are given in Table 1.

Model for SST at time and location of hurricane

This study proposes a model for the SST at the place and location of the hurricane, T, as a function of climatic conditions, which are synthetically represented by the average yearly SST, T_y. The SST T is assumed to follow a probability distribution with mean and standard deviation described as linear functions of T_y. The linear regression models were developed using the National Oceanic and Atmospheric Administration (NOAA) datasets for T and T_y corresponding to years 1988-2018 (NOAA/OAR/ESRL-

PSD 2015). The obtained relation for the mean SST, μ_T , is plotted in Fig. 2(a) with the historical data and is given by:

$$\mu_T\left(T_y\right) = a_{T0} + a_{T1} \cdot T_y \tag{3}$$

in which $a_{T0} = -27.38\ ^{\circ}\mathrm{C}$ and $a_{T1} = 2.19$. Eq. (3) is valid for $T_y \geq 24.0\ ^{\circ}\mathrm{C}$. The standard deviation was found to be almost independent of T_y, with the slope of the regression line statistically equal to zero (p-value = 0.33). Thus, the SST standard deviation is assumed constant and equal to $\sigma_T = 1.23\ ^{\circ}\mathrm{C}$. Based on the results of a modified Kolmogorov-Smirnov test (Soong 2004), a normal distribution with mean given by Eq. (3) and $\sigma_T = 1.23\ ^{\circ}\mathrm{C}$ is selected to describe T .

Peak wind speed model

A statistical model for $V_{\max}$ as a function of T was developed based on the historical peak hurricane wind speeds collected from the HURDAT2 database (Landsea et al. 2015) and the maximum temperature at the time and location of the hurricane obtained from the NOAA database (NOAA/OAR/ESRL-PSD 2015) for hurricanes in the Atlantic Basin during the period 1988-2018. The historical data of $V_{\max}$ are plotted as a function of T in Fig. 2(b) together with the linear regression model used to describe $\mu_{V_{\max}}\left(T\right)$. The regression parameters for the mean and standard deviation of $V_{\max}$ according to Eqs. (1) and (2) (as well as the p-values of the slopes of the regressions) are given in Table 2 and are valid for $T \geq 24^{\circ}\mathrm{C}$. Based on the results of a two-sided Kolmogorov-Smirnov test (Soong 2004), the Weibull distribution provides the best fit to the collected data and is adopted here, consistently with other research works available in the literature (e.g., Li and Ellingwood 2006).

Radius to maximum wind speed model

The statistical model for $R_{\max}$ was developed using the same approach and the same data sources used for $V_{\max}$. The historical data of $R_{\max}$ are plotted as a function of T in Fig. 2(c) together with the linear regression model used to describe $\mu_{R_{\max}}\left(T\right)$. The regression parameters for the mean and standard deviation of $R_{\max}$ according to Eqs. (1) and (2) (as well as the p-values of the slopes of the regressions) are given in

Table 2 and are valid for $T \geq 24^{\mathrm{o}}\mathrm{C}$. Based on the results of a two-sided Kolmogorov-Smirnov test (Soong 2004), the truncated normal distribution with lower tail truncation $R_{\max} > 0$ provides the best fit to the collected data and is adopted here, consistently with other research works available in the literature (Bjarnadottir et al. 2011; Unnikrishnan and Barbato 2017). A weak but not negligible inverse correlation between for $V_{\max}$ and $R_{\max}$ was also found, with a correlation coefficient $\rho_{V_{\max} R_{\max}} = -0.301$.

Translational wind speed model

The statistical model for V_{t} was developed following a similar approach and the same data sources used for $V_{\max}$ and $R_{\max}$. Because the values of V_{t} are not directly available in the HURDAT2 database (Landsea et al. 2015), they were calculated as the maximum values of the translational speed along each hurricane track by assuming a constant translational speed between subsequent recorded positions of the tropical cyclone center. Fig. 2(d) shows the historical data for V_{t} and the linear regression fit for the mean of V_{t} as a function of T. The slopes of the linear regressions for mean and standard deviation of V_{t} are not statistically different than zero (see Table 2); thus, both mean and standard deviation of V_{t} are assumed to be independent of T. Based on the results of a two-sided Kolmogorov-Smirnov test (Soong 2004), a log-normal distribution with $\mu_{V_{\mathrm{t}}} = 6.02\ \mathrm{m/s}$ and $\sigma_{V_{\mathrm{t}}} = 2.45\ \mathrm{m/s}$ provides the best fit to the collected data and is adopted here. It is noteworthy that V_{t} is a variable that is location-dependent, with hurricanes generally moving faster north along the Atlantic Coast region and moving slower inside the Gulf Coast region (Vickery and Twinsdale 1995; Vickery et al. 2000). However, a single random variable is used here to describe the hurricane translation wind speed over the entire US Gulf and Atlantic Coast region. In fact, this quantity has a small effect on the peak wind speeds, which represent the focus of this study. This modeling assumption is not appropriate when modeling other hazards such as storm surge and rainfall, which are strongly dependent on the translational wind speed of tropical cyclones. For these applications, it is recommended to use multiple location-dependent random variables to describe V_{t}.

Development of hurricane wind speed distributions for the US Gulf and Atlantic Coast as function of climatological conditions

A simulation approach based on a multi-layered Monte Carlo simulation (Barbato et al. 2013; Unnikrishnan and Barbato 2017) is proposed here to develop the hurricane wind speed distributions at different locations as functions of climatological conditions described by changes in the SST. A flowchart of the simulation algorithm is provided in Fig. 3. The random parameters used in the sampling procedure and their probability distributions are described in Table 3.

The methodology is initialized by selecting the location (latitude and longitude) of the site of interest, the number of samples, n_s, and the year of interest, y. Once the locations is selected, the corresponding value of ν_{h} is obtained from the NIST database (NIST 2016). The sampling procedures is started by finding the average yearly SST, $T_y^{(i)}$, for sample *i*. If the simulation is done to validate historical data (in this study, when $y \leq 2005$), $T_y^{(i)}$ is set deterministically equal to the measured average yearly SST for the year under consideration, e.g., by using data from NOAA's records (NOAA/OAR/ESRL-PSD 2015). If the simulation is performed to predict future wind speed distributions for a given scenario, the temperature increment $\Delta T_y^{(i)}$ is sampled based on the data reported in the IPCC AR5 (Stocker et al. 2013). These data correspond to the mean and the 90% confidence intervals for the predicted global annual SST changes during the 2010-2060 period with respect to 2005, which are reported in Fig. 4. In particular, the filled markers represent the mean estimates, whereas the empty markers correspond to the lower and upper bounds of the 90% confidence intervals. This figure also shows the estimated global annual SST change for years 2010 and 2015 with respect to year 2005. The lower and upper bounds of the 90% confidence intervals for the measured ΔT_y in 2010 and 2015 are not visible at the scale used in Fig. 4 and are equal to [0.25, 0.29] °C for 2010 and [0.38, 0.42] °C for 2015. The IPCC AR5 projections do not provide the probability distribution for the average yearly SST increase. In the present study, the average yearly SST change in any given year is assumed to follow a truncated normal distribution (with the lower bound equal to -1.73 °C) fitted to data corresponding to the different IPCC AR5 projections (Stocker et al. 2013). The *i*-th sample value of T_y for the year and scenario of interest is finally obtained as:

$$T_y^{(i)} = T_{2005} + \Delta T_y^{(i)} \tag{4}$$

in which, $T_{2005} = 25.73\ ^{\circ}\mathrm{C}$ is the average yearly SST for the reference year 2005 used by the IPCC AR5 projection scenarios. The lower bound of the ΔT_y distribution was selected so that $T_y \geq 24\ ^{\circ}\mathrm{C}$, consistently with the validity range for Eq. (3).

The next step of the sampling procedure requires sampling the number of hurricanes in a year for the *i*-th sample, $n_\mathrm{h}^{(i)}$, from a Poisson distribution with an event rate equal to ν_h for the location of interest. If $n_\mathrm{h}^{(i)} = 0$, the yearly maximum wind speed for the *i*-th sample is set equal to zero, i.e., $V^{(i)} = 0\ \mathrm{m/s}$. Otherwise, an inner loop is initiated to obtain the maximum wind speeds for each of the sampled hurricanes in a year corresponding to the *i*-th sample.

For the *j*-th hurricane of this inner loop (where $j = 1, 2, \ldots, n_\mathrm{h}^{(i)}$), the sampling procedure requires to sample the position of the hurricane eye closest to the location of interest, conditional to this position being on water. More specifically, a bearing angle, $\theta^{(i,j)}$, and a distance, $r^{(i,j)}$, are sampled from a uniform distribution and a truncated generalized extreme value distribution (tGEV) respectively, as described in Table 3. The values of the parameters defining the tGEV distribution (i.e., radius of influence r_{inf}, location parameter λ, scale parameter κ, and shape parameter ξ) are given in Table 1 for the different locations considered in this study (see Fig. 1(b)). The values of r_{inf} were calculated using historical hurricane tracks for mileposts along the US Gulf and Atlantic Coast at intervals of 185.2 km (100 nautical miles) by using the HURDAT2 database (Landsea et al. 2015) and considering all the hurricanes in the Atlantic basin during the period 1871-1963, i.e., the period for which the NIST database was developed (Batts et al. 1980). In particular, the values of r_{inf} were obtained by rounding to the next 10 km the distance within which the hurricane frequency obtained from historical data coincides with the hurricane annual frequency provided by the NIST database, ν_h. The values of the other parameters were obtained by fitting a tGEV distribution to the historical data from the HURDAT2 database (Landsea et al. 2015). Only hurricane location samples positioned on water are accepted by digitizing the map of the region and rejecting the location samples on land until the condition is satisfied. The procedure to identify the hurricane eye's position from the latitude and longitude of the site on interest and the sampled values of r and θ is described in Todhunter (2006).

Once the hurricane eye's position is determined, the temperature $T^{(i,j)}$ at the time and location of the hurricane is sampled from a truncated normal distribution with lower limit equal to 24 °C, mean $\mu_T\left(T_y^{(i)}\right)$ obtained from Eq. (3), and standard deviation $\sigma_T = 1.23\ ^{\circ}\mathrm{C}$. The probability distributions shown in Table 3 are used in combination with the Nataf's model (Liu and Der Kiureghian 1986) to sample the remaining IM components $V_{\max}^{(i,j)}$, $R_{\max}^{(i,j)}$, and $V_{\mathrm{t}}^{(i,j)}$, with correlation coefficients $\rho_{R_{\max},V_{\max}} = -0.301$ and $\rho_{V_{\max},V_{\mathrm{t}}} = \rho_{R_{\max},V_{\mathrm{t}}} = 0$. The parameter values given in Table 2 are used in conjunction with Eq. (1) to determine $\mu_{V_{\max}}\left(T^{(i,j)}\right)$ and $\mu_{R_{\max}}\left(T^{(i,j)}\right)$, and with Eq. (2) to determine to determine $\sigma_{V_{\max}}\left(T^{(i,j)}\right)$ and $\sigma_{R_{\max}}\left(T^{(i,j)}\right)$.

The next step of the sampling procedure requires to calculate the pressure gradient component of the wind speed, $V_{\mathrm{r}}^{(i,j)}$, which in this study is based on the Willoughby's model for dual-exponential hurricane profile (Willoughby et al. 2006). This model is a piecewise continuous profile for the pressure gradient component of the hurricane wind speed defined as follows (Fig. 5):

$$V_{\mathrm{r}}(r) = \begin{cases} V_1 = V_{\max} \cdot \left(\dfrac{r}{R_{\max}}\right)^n & 0 \le r \le R_1 \\ V_1 \cdot (1-w) + V_2 \cdot w & R_1 < r < R_2 \\ V_2 = V_{\max} \cdot \left[(1-A) \cdot e^{\left(-\frac{r-R_{\max}}{X_1}\right)} + A \cdot e^{\left(-\frac{r-R_{\max}}{X_2}\right)}\right] & r \ge R_2 \end{cases} \tag{5}$$

where n is the exponent controlling the wind speed increase inside the hurricane eye, w denotes a weighting function described by a smooth 9th order polynomial that monotonically increases from zero to one in the transition zone defined by $R_1 \le R_{\max} \le R_2$, X_1 and X_2 denote the e-folding lengths, and A is a parameter determining the proportion of the two exponentials in the profile outside the transition zone. Based on Willoughby et al. (2006), $R_2 = R_1 + 10\ \mathrm{km}$, $X_2 = 25\ \mathrm{km}$, whereas n, X_1, and A are correlated random variables described by the probability distributions given in Table 3 with correlation coefficients $\rho_{X_1 n} = -0.143$, $\rho_{X_1 A} = 0.165$, and $\rho_{nA} = 0.391$. These distributions were obtained by fitting to the data provided for the dual-exponential model in Willoughby et al. (2006). Also in this case, the statistical sampling of the correlated random variables n, X_1, and A is performed using the Nataf's model (Liu and Der Kiureghian 1986). Parameter R_1 is a function of n, A, X_1, X_2, and $R_{\max}$ and is found by numerical inversion of the 9th order polynomial defining w after calculating the value of w corresponding to $V_{\max}$ (Willoughby et al. 2006).

Finally, the heading angle $\beta^{(i,j)}$ is sampled from a normal distribution with mean and standard deviation derived from historical data (Vickery et al. 2000). Using the Georgiou's model (Georgiou et al. 1983), the sampled pressure gradient and translational wind speeds, $V_{\mathrm{r}}^{(i,j)}$ and $V_{\mathrm{t}}^{(i,j)}$, are combined to obtain the maximum gradient wind speed at the site of interest, $V^{(i,j)}$:

$$V^{(i,j)} = \frac{1}{2} \cdot \left[V_{\mathrm{t}}^{(i,j)} \cdot \sin\left(\alpha^{(i,j)}\right) - f \cdot r^{(i,j)} \right] + \sqrt{\frac{1}{4} \cdot \left[V_{\mathrm{t}}^{(i,j)} \cdot \sin\left(\alpha^{(i,j)}\right) - f \cdot r^{(i,j)} \right]^2 + \left(V_{\mathrm{r}}^{(i,j)} \right)^2} \tag{6}$$

in which $\alpha^{(i,j)}$ is the relative angle between the translational direction of the hurricane (defined by the heading angle $\beta^{(i,j)}$) and the direction defined by connecting the site of interest with the hurricane eye position, and f is the Coriolis parameter.

The simulated hurricane wind speeds obtained using the proposed sampling procedure can then be post-processed depending on the statistics of interest. For example, if the statistics of interest is the annual peak wind speed distribution at the site, the experimental cumulative distribution function can be obtained by using only the yearly maxima, i.e., $V^{(i)} = \max_{1 \le j \le n_{\mathrm{h}}^{(i)}} \left(V^{(i,j)} \right)$. It is also noted that the hurricane wind speed obtained from the proposed sampling procedure correspond to the fastest 1-minute hurricane speed at 10 m above ground over open terrain, i.e., equivalent to Exposure Category C in ASCE 7-16 (ASCE 2016). The simulated hurricane wind speeds V can then be converted to different gust averaging times, exposures, and elevations as follows:

$$V_{t,e,z} = c_t \cdot c_e \cdot c_z \cdot V \quad (7)$$

where c_t = conversion factor for different wind time averages (ESDU 1993, ASCE 2016) with $c_t = 1$ for the fastest 1-minute hurricane speed, c_e = conversion factor for different terrain exposure categories (ASCE 2016) with $c_e = 1$ over open terrain (Exposure Category C), and c_z = conversion factor for different elevations z above ground (ASCE 2016) with $c_z = 1$ at z = 10 m above ground.

Validation of the proposed model with historical data

The proposed simulation procedure for the hurricane wind speed at a given location along the US Gulf and Atlantic Coast is validated by comparing the statistics of the simulation results with two sets of historical data: hurricane wind speeds from the NIST database (NIST 2016), and design wind speeds from ASCE 7-16 (ASCE 2016). The first set of data from the NIST database (NIST 2016) is used to validate the means and the standard deviations (i.e., the body region of the corresponding distribution) of historical hurricane wind speeds during the 1871-1963 period for the considered mileposts. The simulation procedure was performed using as T_y the average value of the annual temperature for this period, i.e., $T_{1871\text{-}1963} = 25.41\,^{\circ}$C. The NIST data corresponds to fastest 1-minute hurricane speeds at 10 meters above ground over open terrain; thus, for this comparison, the coefficients in Eq. (7) assume the values $c_t = c_e = c_z = 1.0$. The results from the proposed simulation method are based on 1,000,000 samples and are compared with the means and standard deviations obtained from the 999 data points available at each location from the NIST database. These means and standard deviations are conditional to the occurrence of a hurricane event. Fig. 6(a) and (b) compare the means and standard deviations, respectively, obtained from the NIST data and the proposed model at each considered milepost from the coast of Texas to that of Maine. The 95% confidence intervals for the estimates of the means and standard deviations are also shown, even though those corresponding to the simulated data from the proposed simulation method are not visible at the scale presented in Fig. 6.

Table 4 reports the hurricane wind speed means and standard deviations estimated using the NIST data and the simulated data obtained from the proposed method, as well as the corresponding percent relative errors, for all the considered mileposts along the US Gulf and Atlantic Coast. The average relative difference between the simulated and NIST estimates of the hurricane wind speed means is +0.68%, with individual relative differences contained between -1.79% and 3.33%. The corresponding root mean square error (RMSE) and the modified root mean square error (mRMSE) (Peng et al. 2014; Rizzo et al. 2018) for the hurricane wind speed means are equal to $0.33\,\mathrm{m/s}$ and $0.00\,\mathrm{m/s}$, respectively. These results indicate that the proposed simulation procedure is able to reproduce very accurately historical data corresponding to hurricane wind speed means along the entire US Gulf and Atlantic Coast. In fact, the mRMSE value of zero indicates that the simulation estimates of the hurricane wind speed means is always contained within ± 2 standard errors from the NIST-based estimates of the means. The difference between the simulated and NIST estimates of the hurricane wind speed standard deviations is +0.07%, with individual relative errors contained between -21.65% and 21.58%. The corresponding RMSE and mRMSE are equal to $0.83\,\mathrm{m/s}$ and $0.57\,\mathrm{m/s}$, respectively. The proposed simulation procedure generates estimates of hurricane wind speed standard deviations that are globally representative of the US Gulf and Atlantic Coast; however, it can capture well the effects of geographical differences for the hurricane wind speed means, but not for the hurricane wind speed standard deviations, as observed from Fig. 6.

The second set of data from the design wind speeds given in ASCE 7-16 (ASCE 2016) is used to validate the tail of the hurricane wind speed distributions. In particular, the ASCE 7-16 design wind speeds (also referred to as basic wind speeds) correspond to the 3-second gust wind speeds over open terrain at 10 m above ground at any given location with mean return intervals (MRIs) of 300, 700, 1700, and 3000 years, which are used for the design of structures of risk category I through IV, respectively. Thus, the coefficients in Eq. (7) assume the values $c_e = c_z = 1.0$ and $c_t = 1.25$. The design wind speeds in ASCE 7-16 are based on data corresponding to the 1886-1983 period, for which the average yearly SST was calculated as $T_{1886\text{-}1983} = 25.30^{\mathrm{o}}\mathrm{C}$. It is noted here that the design wind speed in ASCE 7-16 are obtained from the wind speed distributions including both hurricane and non-hurricane wind speeds, whereas the wind speeds obtained from the proposed simulation procedure correspond to the hurricane wind speeds only. However, it was also observed that the differences between the two distributions in all the locations considered in this study are negligible for MRI larger than or equal to 100 years. The design wind speeds obtained from the proposed sampling methodology are based on 1,000,000 simulations and are obtained as:

$$V_{MRI} = \mathrm{CDF}^{-1}\left(\frac{MRI-1}{MRI}\right) \tag{8}$$

in which, MRI = 300, 700, 1700, and 3000 years denotes the MRI of interest, and CDF^{-1} denotes the inverse of the empirical cumulative distribution function (CDF) of the generated wind speed data. Table 5 reports the wind speeds corresponding to MRIs of 300, 700, 1700, and 3000 years obtained from ASCE 7-16 and from the proposed simulation procedure at each considered milepost from the coast of Texas to that of Maine, as well as the relative differences between the two sets of values. As shown in Table 5, the average relative differences in the design wind speeds over all mileposts are smaller than 1% in absolute value for all four risk categories, with minimum and maximum relative differences slightly increasing in absolute values for increasing MRIs. The RMSEs over all considered mileposts for structures corresponding to risk categories I through IV are equal to 1.80 m/s, 2.55 m/s, 2.84 m/s and 3.07 m/s, respectively. It is observed that the proposed simulation procedure can match very well the design wind speeds overall, with only a few locations out of the 27 considered along the US Gulf and Atlantic Coast where the simulated design wind speeds differ from the ASCE 7-16 design wind speeds by more than 5% (i.e., in 5, 7, 3, and 4 locations for MRIs of 300, 700, 1700, and 3000 years, respectively). These locations correspond almost exactly to the locations where higher differences were observed between the NIST-based and the simulated estimates of the hurricane wind speed standard deviations. It is also observed that the average relative differences and the RMSEs of the simulated design wind speed tend to slightly increase for increasing MRIs. Based on the results presented here, it is shown that the proposed simulation approach can capture well both the body and the tail of the hurricane wind speed distributions obtained from historical data for different locations along the US Gulf and Atlantic Coast.

Hurricane wind speed projections considering climate change: comparison with other existing models and design implications

The proposed simulation procedure is used to develop projected hurricane wind speed distributions under different climate change projections along the US Gulf and Atlantic Coast. As a further validation of this methodology, its projection results are compared with those obtained from existing methodologies based on a rigorous simulation of the hurricane tracks from their formation in the Atlantic Ocean to their landfall on the US Gulf and Atlantic Coast based on downscaled climate change projections. Specifically, the wind speed projections for year 2100 in Miami, FL, corresponding to the models developed by Cui and Caracoglia (2016) and Pant and Cha (2019) are compared in Fig. 7 to those obtained using the proposed model for the climate change scenarios defined by the best case scenario RCP 2.6 and the worst case scenario RCP 8.5. The predicted changes in design wind speeds obtained by using the proposed model are very close to those provided by the other two models, with a maximum absolute value of the relative differences smaller than 3.0% for the RCP 2.6 scenario (corresponding to a wind speed difference of approximately 2.3 m/s) and smaller than 2.4% for the RCP 8.5 scenario (corresponding to a wind speed difference of approximately 2.2 m/s). It is concluded that the proposed simulation procedure provides projections of wind speed distributions that are consistent with other existing methodologies based on hurricane tracks at a small fraction of their computational cost. For example, the proposed methodology allows to derive the hurricane wind speed distributions based on 1,000,000 simulation at the 27 different locations and for all four climate change scenarios considered in this study in little less than 2 minutes on an ordinary personal computer (Intel® Core i7-8700 processor, 3.2 GHz, 16 GB RAM).

Finally, the proposed simulation approach is used to estimate the projected wind design speeds under different climate change scenarios at different locations along the US Gulf and Atlantic Coast. Table 6 reports the projected absolute and relative increases in design wind speeds by year 2060 at each considered milepost from the coast of Texas to that of Maine when considering the RCP 8.5 climate change scenario. These average relative increases in design wind speeds are equal to 25.01%, 24.52%, 25.13%, and 26.05% for structures in risk categories I through IV, respectively, with peak relative increases as high as 39.70% near the coast of Maine, where the largest relative increases are expected for all risk categories.

Similar results for other climate change scenarios are not reported here due to space constraints, but the following average relative increases in the design wind speeds are obtained for the four risk categories considered in ASCE 7-16: (1) 14.52%, 14.00%, 14.47%, and 15.27% for RCP 2.6; (2) 18.87%, 18.32%, 18.96%, and 19.82% for RCP 4.5; and (3) 17.87%, 17.39%, 17.97%, and 18.87% for RCP 6.0. Because the design wind force applied on a structure increases quadratically with the design wind speed, these results suggest that, in order to maintain the same reliability required by the current ASCE 7-16 design code under wind loads, structures with a design life longer than 50 years and located along the US Gulf and Atlantic Coast should be designed for a larger wind force than that used today, with an increase of at least 30% for RCP 2.6, at least 40% for RCP 4.5 and RCP 6.0, and between 55% and 59% for RCP 8.5.

Conclusions

This paper proposes a novel and efficient simulation methodology based on historical records to predict hurricane wind speed statistics under different climatological conditions. The developed procedure allows to simulate hurricane wind speeds at any given location along the US Gulf and Atlantic Coast by considering the effects of climate change. The newly developed simulation procedure was validated versus historical data from NIST and the design wind speeds provided in ASCE 7-16. In addition, the results of the proposed simulation approach were compared with those obtained using other existing procedures requiring the simulation of the full tracks of hurricanes. The obtained hurricane wind speed projections were found to be consistent (i.e., less than 3.5% absolute relative differences) with those of these other methods, while being significantly less computationally expensive (i.e., with a computational time of the order of minutes on an ordinary personal computer). The simulation procedure was used in conjunction with the projection scenarios given in the Intergovernmental Panel on Climate Change's 5th Assessment Report to simulate hurricane wind speeds corresponding to mean return intervals of 300, 700, 1700, and 3000 years (i.e., corresponding to the design wind speeds for buildings belonging to risk category I, II, III, and IV in ASCE 7-16) under possible future climatological conditions. The simulation results indicate that climate change could produce significant changes in the design wind speeds in the next 40-100 years. In particular, by 2060, the design wind speeds along the US Gulf and Atlantic Coast are projected to increase between approximately 14% (for risk category II under scenario RCP 2.6) and 26% (for risk category IV under scenario RCP 8.5), which correspond to an average increase of the wind force acting on a structure between approximately 30% and 59%. Therefore, it is suggested to include climate change effects in the development of design wind maps for structures with extended design life in future version of ASCE 7.

Finally, whereas the model presented in this study is specifically developed for the US Gulf and Atlantic Coast, the same methodology can be employed for other hurricane-prone regions worldwide, by using the appropriate historical records to fit the numerical values of the parameters used in the present model.

The wind speed model developed in this study provides an invaluable tool for further investigation of climate change effects on the performance of the US built environment and national infrastructure systems. An important aspect that needs to be quantified in future studies is the effect of epistemic uncertainties, e.g., through a sensitivity analysis and/or a probability bounds analysis of the wind speed estimates with respect to the adopted probability distributions, the statistics used to describe such distributions, and the likelihood of different climate scenarios. Another essential research need is the quantification of the effects of the predicted wind force increases on the performance of structural and infrastructural systems, with the resulting implications on future design and building codes for different types of structures ranging from single-family houses and residential/non-residential buildings to critical infrastructure components such as bridges, dams, levees, communication towers, and power plants. Finally, the proposed wind model, used in conjunction with the results of the suggested structural performance studies, could inform the next generation of catastrophe models to predict the effects of climate change in terms of economic and life losses, to assess the resilience of our infrastructure, to quantify the potential societal impact, and above all to propose feasible mitigation and adaptation strategies that could be implemented in both the short- and long-term.

Data Availability Statement

All data, models, or code that support the findings of this study are available from the corresponding author upon reasonable request.

References

Adams, C., Hernandez, E., and Cato, J. C. (2004). "The economic significance of the Gulf of Mexico related to population, income, employment, minerals, fisheries and shipping." *Ocean & Coastal Management*, 47(11–12): 565–580.

ASCE (2016). *ASCE/SEI 7: Minimum Design Loads and Associated Criteria for Buildings and Other*

Structures. American Society of Civil Engineers, Reston, VA, USA.

Barbato, M., Petrini, F., Unnikrishnan, V. U., and Ciampoli, M. (2013). "Performance-Based Hurricane Engineering (PBHE) framework." *Structural Safety*, 45, 24-35.

Batts, M. E., Russell, L. R., and Simiu, E. (1980). "Hurricane wind speeds in the United States." *Journal of the Structural Division*, 106(10): 2001-2016.

Bjarnadottir, S., Li, Y., and Stewart, M. G. (2011). "A probabilistic-based framework for impact and adaptation assessment of climate change on hurricane damage risks and costs." *Structural Safety*, 33(3): 173–185.

Bjarnadottir, S., Li, Y., and Stewart, M. G. (2014). "Regional loss estimation due to hurricane wind and hurricane-induced surge considering climate variability." *Structure and Infrastructure Engineering*, 10(11): 1369–1384.

Crossett, K., Ache, B., Pacheco, P., and Haber, K. (2013). *National coastal population report: Population trends from 1970 to 2010*. NOAA State of the Coast Report Series, US Department of Commerce, Washington, DC, USA.

Cui, W., and Caracoglia, L. (2016). "Exploring hurricane wind speed along US Atlantic coast in warming climate and effects on predictions of structural damage and intervention costs." *Engineering Structures*, 122: 209–225.

Elsner, J. B, Lewers, S. W., Malmstadt, J. C. and Jagger, T. H. (2011). "Estimating contemporary and future wind-damage losses from hurricanes affecting Eglin Air Force Base, Florida". *Journal of Applied Meteorology and Climatology*, 50(7): 1514-1526.

Elsner, J. B, Trepanier, J. C., Strazzo, S. E., and Jagger, T. H. (2012). "Sensitivity of limiting hurricane intensity to ocean warmth". *Geophysical Research Letters*, 39: L17702.

Emanuel, K. (2011). "Global warming effects on U.S. hurricane damage." *Weather, Climate, and Society*. 3(4): 261–268.

Emanuel, K. (1999). "Thermodynamic control of hurricane intensity." *Nature*, 401: 665–669.

Engineering Sciences Data Unit (ESDU) (1993). *Strong winds in the atmospheric boundary layer, Part 2:*

Discrete gust speeds. ESDU 83045, London, UK.

Georgiou P. N., Davenport A. G., and Vickery B. J. (1983). “Design wind speeds in regions dominated by tropical cyclones.”, *Journal of Wind Engineering and Industrial Aerodynamics*, 13(1-3): 139-152.

Grinsted, A., Moore, J. C., and Jevrejeva, S. (2013). “Projected Atlantic hurricane surge threat from rising temperatures.” *Proceedings of the National Academy of Sciences*, 110(14): 5369–5373.

Hallegatte, S. (2007). “The use of synthetic hurricane tracks in risk analysis and climate change damage assessment.” *Journal of Applied Meteorology and Climatology*, 46(11): 1956–1966.

Huang, Z., Rosowsky, D. V., and Sparks, P. R. (2001). “Hurricane simulation techniques for the evaluation of wind-speeds and expected insurance losses.” *Journal of Wind Engineering and Industrial Aerodynamics*, 89(7–8): 605–617.

Jagger, T. H., Elsner, J. B., and Niu, X. (2001). “A dynamic probability model of hurricane winds in coastal counties of the United States”. Journal of Applied Meteorology, 40(5): 853-863.

Jagger, T. H., and Elsner, J. B. (2012). “Hurricane clusters in the vicinity of Florida”. *Journal of Applied Meteorology and Climatology*, 51(5): 869-877.

Knutson, T. R., McBride, J. L., Chan, J., Emanuel, K., Holland, G., Landsea, C., Held, I., Kossin, J. P., Srivastava, A. K., and Sugi, M. (2010). “Progress article: Tropical cyclones and climate change.” *Nature Geoscience*, 3(3): 157–163.

Knutson, T. R., Sirutis, J. J., Garner, S. T., Held, I. M., and Tuleya, R. E. (2007). “Simulation of the recent multidecadal increase of Atlantic hurricane activity using an 18-km-grid regional model.” *Bulletin of the American Meteorological Society*, 88(10): 1549–1565.

Knutson, T. R., Sirutis, J. J., Vecchi, G. A., Garner, S., Zhao, M., Kim, H. S., Bender, M., Tuleya, R. E., Held, I. M., and Villarini, G. (2013). “Dynamical downscaling projections of twenty-first-century atlantic hurricane activity: CMIP3 and CMIP5 model-based scenarios.” *Journal of Climate*, 26(17): 6591–6617.

Landsea, C., Franklin, J., and Beven, J. (2015). “The revised Atlantic hurricane database (HURDAT2).” Accessed March 17, 2018. http://www.aoml.noaa.gov/hrd/hurdat/hurdat2.html.

Lee, J. Y., and Ellingwood, B. R. (2017). “A decision model for intergenerational life-cycle risk assessment of civil infrastructure exposed to hurricanes under climate change.” *Reliability Engineering and System Safety*, 159:100-107.

Li, Y., and Ellingwood, B. R. (2006). “Hurricane damage to residential construction in the US: Importance of uncertainty modeling in risk assessment.” *Engineering Structures*, 28(7): 1009–1018.

Liu, P. L., and Der Kiureghian, A. (1986). “Multivariate distribution models with prescribed marginals and covariances.” *Probabilistic Engineering Mechanics*, 1(2): 105–112.

Lombardo, F. T. and Ayyub, B. M. (2015). “Analysis of Washington, DC, wind and temperature extremes with examination of climate change for engineering applications.” *Journal of Risk Uncertainty in Engineering Systems. Part A: Civil Engineering*, 1(1): 04014005.

Malmstadt, J. C, Elsner, J. B., and Jagger, T. H. (2010). “Risk of strong hurricane winds to Florida cities”. *Journal of Applied Meteorology and Climatology*, 49(10): 2121-2132.

Manuel, K., Sundararajan, R., and Williams, J. (2008). “Hurricanes and global warming: Results from downscaling IPCC AR4 simulations.” *Bulletin of the American Meteorological Society*, 89(3): 347–367.

Mudd, L., Wang, Y., Letchford, C., and Rosowsky, D. (2014). “Assessing climate change impact on the U.S. East Coast hurricane hazard: Temperature, frequency, and track.” *Natural Hazards Review*, 15(3), 04014001.

National Hurricane Center (2018). “Costliest U.S. tropical cyclones tables updated.” *NOAA Technical Memorandum NWS NHC-6*: 1-3, NOAA Silver Spring, MD, USA.

NIST. (2016). “Extreme wind speed data sets: Hurricane wind speeds.” Accessed March 17, 2018. http://www.itl.nist.gov/div898/winds/hurricane.htm

NOAA/OAR/ESRL-PSD. (2015). “NOAA high resolution SST data.” Accessed March 25, 2018. http://www.esrl.noaa.gov/psd/.

Oxenyuk, V., Gulati, S., Kibria, B. M. G., and Hamid, S. (2017). Distribution fits for various parameters in the Florida Public Hurricane Loss model. *Journal of Modern Applied Statistical Methods*, 16(1): 481-497.

Pant, S., and Cha, E. J. (2018). “Effect of climate change on hurricane damage and loss for residential buildings in Miami-Dade County." *Journal of Structural Engineering*, 144(6): 04018057.

Pant, S., and Cha, E. J. (2019). "Wind and rainfall loss assessment for residential buildings under climate-dependent hurricane scenarios." *Structure and Infrastructure Engineering*, 5(6): 771–782.

Peng, X., Yang, L., Gavanski, E., Gurley, K., and Prevatt, D. (2014). "A comparison of methods to estimate peak wind loads on buildings." *Journal of Wind Engineering and Industrial Aerodynamics*, 126: 11–23.

Pielke, R. A., Gratz, J., Landsea, C. W., Collins, D., Saunders, M. A., and Musulin, R. (2008). "Normalized hurricane damage in the United States: 1900–2005." *Natural Hazards Review*, 9(1): 29–42.

Rizzo, F., Barbato, M., and Vincenzo, S. (2018). "Peak factor statistics of wind effects for hyperbolic paraboloid roofs." *Engineering Structures*, 173: 313-330

Soong, T. T. (2004). *Fundamentals of probability and statistics for engineers*. John Wiley & Sons, West Sussex, UK.

Stocker, T. F., Qin, D., Plattner, G.-K., Tignor, M., Allen, S. K., Boschung, J., Nauels, A., Xia, Y., Bex, V., Midgley, P. M., and Others. (2013). *Climate Change 2013 - The Physical Science Basis*. *Contribution of Working Group I to the Fifth Assessment Report of the Intergovernmental Panel on Climate Change*, Cambridge University Press, Cambridge, UK, and New York, NY, USA.

Todhunter, I. (2006). Spherical Trigonometry: For the Use of Colleges and Schools. Mamillan and co., London, UK.

Unnikrishnan, V. U., and Barbato, M. (2017). "Multihazard interaction effects on the performance of low-rise wood-frame housing in hurricane-prone regions." *Journal of Structural Engineering*, 143(8): 04017076

Vickery, P. J., Masters, F. J., Powell, M. D., and Wadhera, D. (2009). "Hurricane hazard modeling: The past, present, and future." *Journal of Wind Engineering and Industrial Aerodynamics*, 97(7–8): 392–405.

Vickery, P. J., Skerlj, P. F., and Twisdale, L. A. (2000). "Simulation of hurricane risk in the US using empirical track model." *Journal of Structural Engineering*, 126(10): 1222-1237.

Webster, P. J., Holland, G. J., Curry, J. A., and Chang, H. R. (2005). "Atmospheric science: Changes in tropical cyclone number, duration, and intensity in a warming environment." *Science*, 309 (5742): 1844-

1846

Willoughby, H. E., Darling, R. W. R., Rahn, M. E. (2006). “Parametric representation of the primary hurricane vortex. Part II: A new family of sectionally continuous profiles.” *Monthly Weather Review*, 134(4), 1102–1120.

Tables

Table 1. Location depedent parameters for mileposts at intervals of 185.2 km (100 nautical miles) along the US Gulf and Atlantic Coast: hurricane annual frequency, ν_{h} ; radius of influence, r_{inf} ; location parameter, λ ; scale parameter, κ ; and shape parameter, ξ

Milepost #	ν_{h} (-)	r_{inf} (km)	λ (km)	κ (km)	ξ (-)
1	0.37	275	215	39.96	-0.71
2	0.44	285	208	41.74	-0.10
3	0.48	270	212	39.13	-0.75
4	0.51	295	223	43.66	-0.36
5	0.50	290	225	42.67	-0.60
6	0.50	295	230	43.56	-0.67
7	0.50	285	220	41.83	-0.56
8	0.51	285	225	41.73	-0.83
9	0.50	295	230	43.96	-0.87
10	0.51	295	235	43.76	-0.92
11	0.51	290	229	37.58	-0.87
12	0.53	225	178	30.99	-0.84
13	0.57	255	192	42.29	-0.40
14	0.55	215	171	42.03	-1.04
15	0.63	300	224	54.67	-0.37
16	0.57	345	268	62.58	-0.69
17	0.53	345	274	62.53	-0.98
18	0.55	320	252	58.66	-0.74
19	0.61	280	221	51.57	-0.46
20	0.68	285	225	51.44	-0.89
21	0.63	268	212	48.29	-0.17
22	0.56	297	234	54.33	-0.65
23	0.45	325	257	58.53	-0.26
24	0.32	307	243	55.48	-0.84
25	0.29	270	213	48.93	-1.01
26	0.29	270	214	48.96	-0.79
27	0.26	292	231	52.85	-0.45

Table 2. Regression parameters for mean and standard deviations of hurricane IMs for the US Gulf and Atlantic Coast

p	Unit	a_{p0}	$a_{p1}\cdot$°C	p-value	b_{p0}	$b_{p1}\cdot$°C	p-value
V_{max}	m/s	-29.31	2.93	0.01	-20.05	1.06	< 0.01
R_{max}	km	105.8	-2.57	0.05	29.0	-0.48	< 0.01
V_{t}	m/s	6.66 (6.02)*	-0.02 (0)*	0.91	-3.52 (2.45)*	0.21 (0)*	0.37

* values in parentheses are those used in the proposed sampling procedure

Table 3. Random variables and corresponding probability distributions used in the proposed sampling procedure

Variable	Unit	Distribution	Distribution description	Range
ΔT_y	°C	Truncated Normal	Based on IPCC AR5 (Stocker et al. 2013) projections	$-1.73 \le \Delta T_y \le +\infty$
n_{h}	-	Poisson	ν_{h} at each location from NIST database (2016)	$n_{\mathrm{h}} \ge 0$
θ	rad	Uniform	$\mu_\theta = \pi, \quad \sigma_\theta = \pi^2/3$	$0 \le \theta \le 2\pi$
r	km	tGEV	Parameters $r_{\mathrm{inf}}, \lambda, \kappa, \xi$ at each location given in Table 1	$0.0 \le r \le r_{\mathrm{inf}}$
T	°C	Truncated Normal	μ_T calculated from Eq. (3), $\sigma_T = 1.23$ °C	$T \ge 24$ °C
$V_{\max}$	m/s	Translated Weibull	$\mu_{V_{\max}}$ calculated from Eq. (1), $\sigma_{V_{\max}}$ calculated from Eq. (2)	$V_{\max} \ge 33.4$ m/s
$R_{\max}$	km	Truncated Normal	$\mu_{R_{\max}}$ calculated from Eq. (1), $\sigma_{R_{\max}}$ calculated from Eq. (2)	$R_{\max} \ge 0.0$ km
V_{t}	m/s	Lognormal	$\mu_{V_{\mathrm{t}}} = 6.02$ m/s, $\sigma_{V_{\mathrm{t}}} = 2.45$ m/s	$V_{\mathrm{t}} \ge 0.0$ m/s
A	-	Mixed GEV	$0.61 + 0.39 \cdot \mathrm{tGEV}(\xi, \kappa, \lambda)$ $\xi = 0.1392, \quad \kappa = 0.1517, \quad \lambda = 0.2044$	$0.0 \le A \le 1.0$
X_1	km	Weighted GEV	$0.82 \cdot \mathrm{tGEV}(\xi_1, \kappa_1, \lambda_1) + 0.18 \cdot \mathrm{tGEV}(\xi_2, \kappa_2, \lambda_2)$ $\xi_1 = -0.0023, \quad \kappa_1 = 65.40, \quad \lambda_1 = 210.55$ $\xi_2 = 0.6519, \quad \kappa_2 = 2.4885, \quad \lambda_2 = 452.41$	$100 \le X_1 \le 500$ km
n	-	Truncated Lognormal	$\mu_n = 0.8808, \quad \sigma_n = 0.4252$	$0.0 \le n \le 2.5$
β	rad	Normal	From Vickery et al. (2000).	$0 \le \beta \le 2\pi$

Table 4. Comparison of hurricane gradient wind speed (fastest 1-minute hurricane speed at 10 m above ground over open terrain) means and standard deviations at different mileposts estimated using NIST data and the proposed simulation procedure

Milepost	NIST (m/s)		Proposed model (m/s)		Relative difference (%)	
#	μ_V	σ_V	μ_V	σ_V	ε_{μ_V}	ε_{σ_V}
1	22.82	9.62	22.60	8.76	-0.97	-8.92
2	22.35	9.17	23.04	8.66	3.10	-5.52
3	23.11	9.46	23.33	8.79	0.95	-7.08
4	21.55	8.44	22.26	8.53	3.30	1.09
5	21.85	8.11	21.81	8.53	-0.18	5.16
6	21.49	8.56	21.39	8.57	-0.48	0.07
7	22.13	9.16	22.27	8.60	0.62	-6.15
8	22.23	8.31	22.10	8.68	-0.59	4.39
9	21.00	7.15	21.70	8.69	3.33	21.58
10	21.74	7.78	21.35	8.70	-1.79	11.80
11	21.54	8.74	21.34	8.49	-0.94	-2.81
12	25.99	8.9	25.86	9.04	-0.49	1.53
13	23.84	10.08	24.36	9.02	2.20	-10.55
14	26.97	9.88	26.63	9.74	-1.24	-1.45
15	21.06	9.13	21.40	8.85	1.60	-3.08
16	18.71	8.57	18.52	8.59	-1.00	0.22
17	17.83	7.92	18.13	8.66	1.70	9.34
18	19.52	9.45	19.57	8.87	0.28	-6.14
19	21.73	9.04	21.90	9.15	0.79	1.24
20	21.19	8.31	21.54	8.97	1.65	7.99
21	22.28	8.93	22.55	9.12	1.21	2.12
22	20.46	7.84	20.83	8.97	1.82	14.38
23	19.07	7.45	19.19	8.77	0.61	17.76
24	20.08	9.21	20.19	8.92	0.57	-3.13
25	22.58	10.87	22.68	8.52	0.44	-21.65
26	22.25	10.15	22.47	9.10	1.01	-10.30
27	20.89	10.00	21.05	8.99	0.79	-10.10
Average	21.71	8.90	21.85	8.82	0.68	0.07
Minimum	17.83	7.15	18.13	8.49	-1.79	-21.65
Maximum	26.97	10.87	26.63	9.74	3.33	21.58

Table 5. Comparison of design wind speeds (base wind speeds corresponding to 3-second gust wind speeds at 10 m above ground over open terrain) from ASCE 7-16 and proposed simulation procedure along the US Gulf and Atlantic Coast

Milepost	ASCE (m/s)				Proposed model (m/s)				Relative difference (%)			
#	300	700	1700	3000	300	700	1700	3000	300	700	1700	3000
1	61.24	66.16	69.74	72.42	58.05	62.73	67.60	70.42	-5.20	-5.18	-3.07	-2.76
2	61.69	66.61	70.63	72.87	58.89	63.19	67.66	70.34	-4.53	-5.13	-4.21	-3.47
3	59.9	64.37	68.4	70.19	60.35	64.92	69.65	72.57	0.75	0.85	1.82	3.39
4	58.12	63.48	68.4	70.19	57.87	62.29	66.54	69.53	-0.43	-1.87	-2.72	-0.93
5	67.06	75.1	80.02	82.7	64.04	68.81	73.85	76.89	-4.50	-8.38	-7.71	-7.02
6	66.61	74.21	80.02	81.81	66.46	71.76	76.86	80.24	-0.23	-3.31	-3.95	-1.92
7	65.27	71.53	78.68	81.81	61.70	66.48	71.06	74.22	-5.47	-7.07	-9.69	-9.27
8	56.77	61.24	66.16	68.4	57.63	62.18	66.87	69.51	1.52	1.54	1.08	1.62
9	52.75	58.56	63.48	62.14	53.79	57.99	62.37	65.10	1.97	-0.98	-1.74	4.77
10	50.52	54.54	60.8	62.14	53.13	57.46	61.61	64.60	5.17	5.35	1.34	3.96
11	59.9	64.82	68.4	70.19	57.44	61.86	66.20	69.07	-4.10	-4.56	-3.21	-1.60
12	64.37	69.29	75.1	78.68	64.66	69.59	74.32	77.27	0.45	0.44	-1.04	-1.79
13	71.53	77.34	82.26	85.83	69.66	74.68	79.61	82.83	-2.62	-3.44	-3.22	-3.50
14	69.29	75.55	80.47	83.6	67.92	73.34	78.82	82.39	-1.98	-2.92	-2.05	-1.45
15	61.24	66.61	71.08	75.55	60.24	64.83	69.28	72.35	-1.63	-2.67	-2.53	-4.24
16	53.64	58.12	62.59	66.61	54.21	58.95	63.62	66.97	1.06	1.43	1.64	0.54
17	52.75	58.12	63.93	67.5	53.03	58.04	63.22	66.54	0.53	-0.14	-1.10	-1.42
18	58.56	65.71	70.19	73.76	57.84	63.00	67.99	71.28	-1.22	-4.13	-3.14	-3.36
19	60.35	66.16	69.74	72.87	60.43	65.40	70.27	73.69	0.12	-1.14	0.77	1.12
20	59.9	64.82	67.95	70.19	59.94	64.57	69.52	72.75	0.06	-0.38	2.31	3.65
21	55.43	59.01	63.03	66.16	55.88	60.27	64.50	67.01	0.81	2.13	2.34	1.29
22	49.62	54.09	58.56	60.8	52.34	56.59	61.03	63.72	5.49	4.63	4.22	4.81
23	50.96	55.88	59.9	62.59	51.81	56.28	60.83	63.85	1.68	0.72	1.56	2.02
24	49.62	54.09	58.56	61.24	50.86	55.77	60.03	63.03	2.51	3.11	2.50	2.93
25	54.09	58.12	62.14	64.37	54.67	58.84	63.13	65.67	1.07	1.24	1.60	2.03
26	54.99	59.01	62.59	64.82	57.16	62.36	67.81	70.94	3.94	5.67	8.35	9.44
27	49.17	53.64	57.22	59.46	52.35	57.43	62.10	65.50	6.46	7.06	8.52	10.15
Average	58.35	63.56	68.15	70.7	58.24	62.95	67.64	70.68	0.06	-0.63	-0.42	0.33
Minimum	49.17	53.64	57.22	59.46	50.86	55.77	60.03	63.03	-5.47	-8.38	-9.69	-9.27
Maximum	71.53	77.34	82.26	85.83	69.66	74.68	79.61	82.83	6.46	7.06	8.52	10.15

Table 6. Projected increases in design wind speeds (basic wind speeds corresponding to 3-second gust wind speeds at 10 m above ground over open terrain) for year 2060 and scenario RCP 8.5 along the US Gulf and Atlantic Coast

Milepost	300 years		700 years		1700 years		3000 years	
#	(m/s)	(%)	(m/s)	(%)	(m/s)	(%)	(m/s)	(%)
1	11.15	18.21	12.22	18.47	14.35	20.58	15.18	20.97
2	12.25	19.86	13.08	19.64	14.36	20.33	15.62	21.43
3	15.62	26.08	17.04	26.46	19.15	28.00	21.00	29.91
4	14.56	25.06	14.75	23.23	15.45	22.58	17.33	24.69
5	11.61	17.31	9.87	13.14	11.48	14.35	12.90	15.60
6	13.93	20.91	12.69	17.11	13.33	16.66	15.89	19.42
7	11.31	17.33	11.09	15.51	9.74	12.38	10.25	12.53
8	15.35	27.03	16.84	27.49	18.02	27.23	19.33	28.26
9	15.44	29.28	15.30	26.13	15.81	24.91	20.28	32.64
10	16.66	32.97	18.18	33.33	17.67	29.06	19.43	31.27
11	12.24	20.44	13.01	20.07	15.15	22.15	17.11	24.37
12	16.91	26.28	18.15	26.19	18.55	24.70	18.51	23.53
13	13.87	19.39	14.76	19.08	16.37	19.90	16.55	19.28
14	16.76	24.19	17.60	23.30	19.83	24.64	21.04	25.17
15	14.46	23.62	15.15	22.74	16.76	23.58	15.52	20.54
16	14.60	27.22	16.09	27.69	18.00	28.76	17.44	26.18
17	13.77	26.11	14.81	25.48	15.66	24.49	16.20	24.00
18	13.90	23.74	13.38	20.36	15.52	22.11	16.21	21.97
19	16.12	26.71	16.71	25.25	19.43	27.86	20.40	28.00
20	15.60	26.04	16.94	26.14	20.30	29.87	22.07	31.45
21	14.85	26.80	16.87	28.59	18.83	29.87	19.50	29.47
22	11.21	22.60	12.15	22.45	12.77	21.80	14.15	23.28
23	14.36	28.18	15.52	27.78	17.24	28.77	18.44	29.46
24	14.30	28.82	16.00	29.58	17.94	30.64	19.41	31.70
25	14.89	27.53	16.63	28.62	18.37	29.57	19.51	30.30
26	16.39	29.81	19.53	33.09	22.36	35.72	24.81	38.28
27	16.62	33.81	18.83	35.10	21.81	38.12	23.60	39.70
Average	14.40	25.01	15.30	24.52	16.82	25.13	18.06	26.05
Minimum	11.15	17.31	9.87	13.14	9.74	12.38	10.25	12.53
Maximum	16.91	33.81	19.53	35.10	22.36	38.12	24.81	39.70

Figures

Fig. 1. US Gulf and Atlantic Coast hurricane-prone region: (a) yearly number of hurricanes in the 1851-2018 period as a function of T_y, and (b) location of mileposts at intervals of 185.2 km (100 nautical miles) considered in this study

Fig. 2. Historical data for US Gulf and Atlantic Coast between 1988-2018 and linear regression lines for: (a) T vs. T_y, (b) $V_{\max}$ vs. T, (c) $R_{\max}$ vs. T, and (d) V_t vs. T

Fig. 3. Flowchart of the proposed hurricane wind speed simulation methodology

Fig. 4. IPCC AR5 Projections for increases in average yearly sea surface temperature

Fig. 5. Description of Willoughby's hurricane profile model

Fig. 6. Comparison of statistics for hurricane wind speed (gradient wind speed corresponding to fastest 1-minute hurricane speeds at 10 meters above ground over open terrain) obtained from the NIST database and from the proposed simulation procedure along the US Gulf and Atlantic Coast: (a) means and (b) standard deviations

Fig. 7. Comparison of projected hurricane wind speeds (gradient wind speeds corresponding to 3-second gust wind speeds at 10 m above ground over open terrain) for year 2100 in Miami, FL, from proposed model, Cui and Caracoglia (2016), and Pant and Cha (2019)

Figure 1

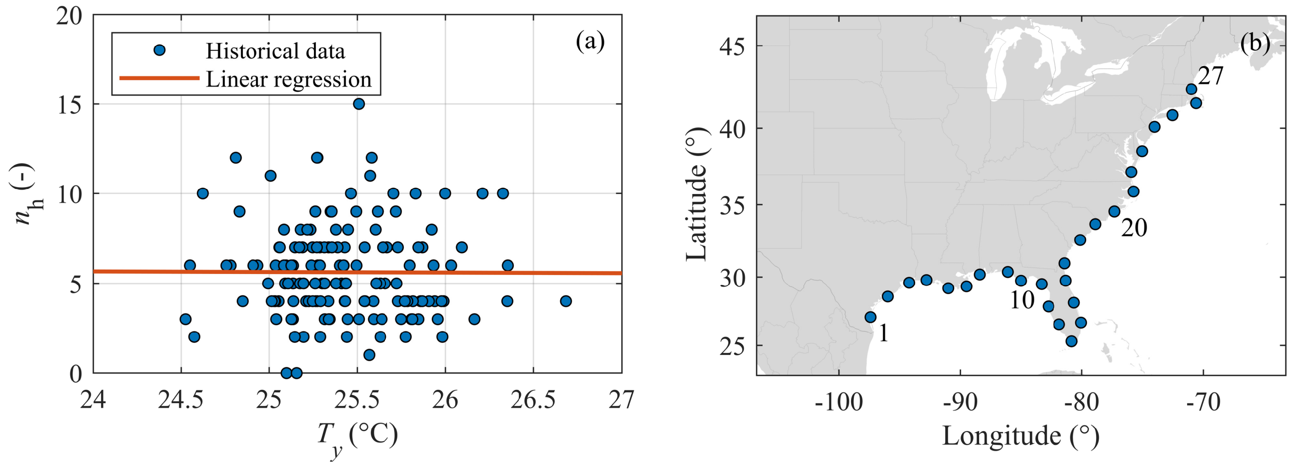

Historical data
Linear regression
(a)
n_h (-)
T_y (°C)
(b)
Latitude (°)
Longitude (°)
1
10
20
27

Figure 2

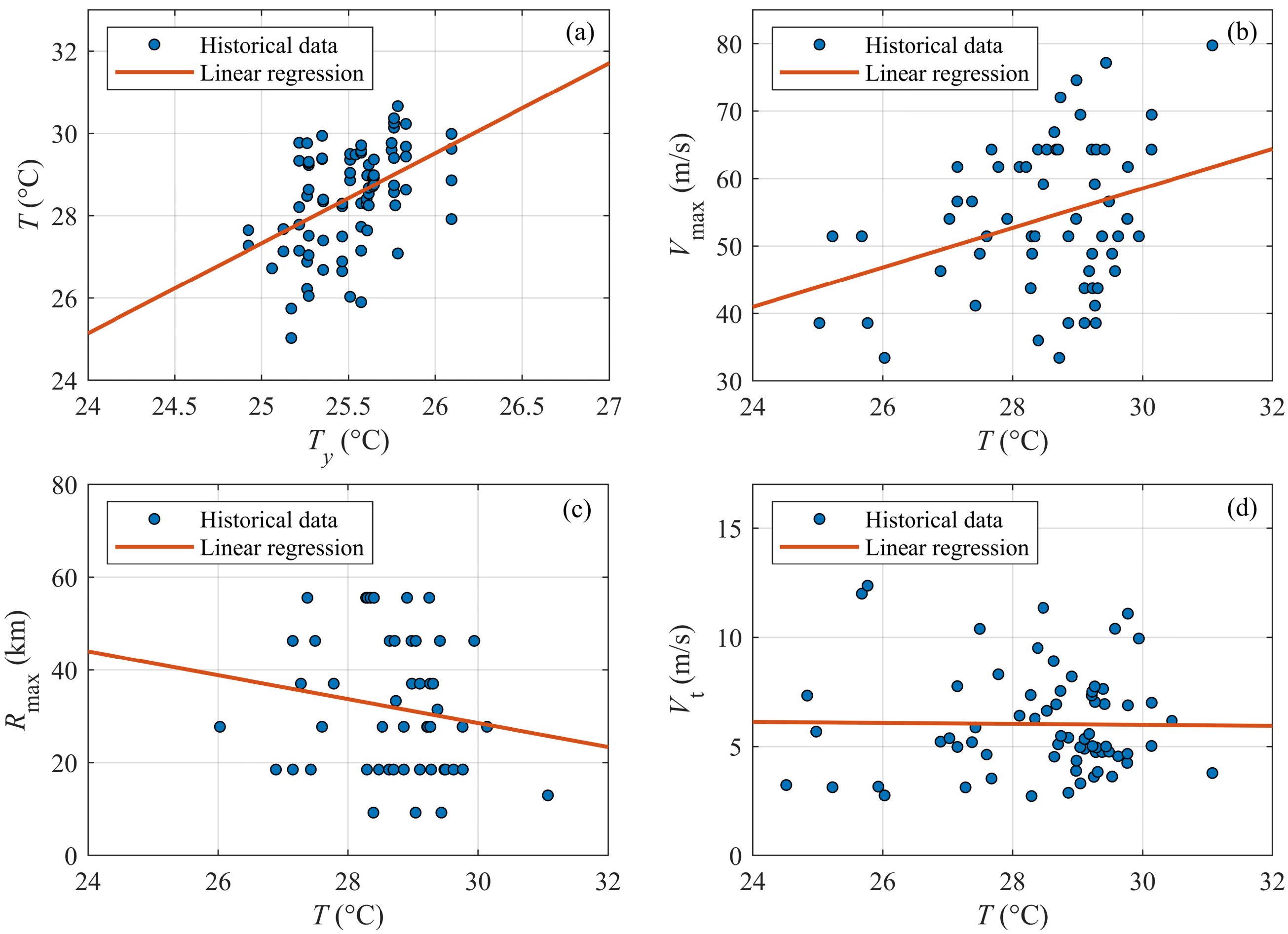
(a)
Historical data
Linear regression
T (°C)
T_y (°C)
(b)
Historical data
Linear regression
V_{max} (m/s)
T (°C)
(c)
Historical data
Linear regression
R_{max} (km)
T (°C)
(d)
Historical data
Linear regression
V_t (m/s)
T (°C)

Figure 3

- Select the site of interest by setting: latitude, longitude, ν_{h}, and r_{inf}.
- Select the number of samples: n_{s}.
- Select the year of interest: y.
- For $i = 1 : n_{\mathrm{s}}$
  - If $y \leq 2005$:
    - Set $T_y^{(i)}$ equal to historical value corresponding to year y.
  - Else
    - Select projection scenario.
    - Sample $\Delta T_y^{(i)}$ from a normal distribution based on IPCC AR5 projections.
    - Calculate $T_y^{(i)}$ from Eq. (4).
  - End if.
  - Sample number of yearly hurricanes, $n_{\mathrm{h}}^{(i)}$, from a Poisson distribution with event rate = ν_{h}.
  - If $n_{\mathrm{h}}^{(i)} = 0$:
    - Set: $V^{(i)} = 0$ m/s
  - Else
    - For $j = 1 : n_{\mathrm{h}}^{(i)}$
      - Sample the hurricane eye location, i.e., bearing angle $\theta^{(i,j)}$, and distance $r^{(i,j)}$ using the distributions given in Table 3. If hurricane eye location is on land, resample until hurricane eye location is on water.
      - Calculate $\mu_T\left(T_y^{(i)}\right)$ from Eq. (3) and sample $T^{(i,j)}$.
      - Calculate $\mu_{V_{\mathrm{max}}}\left(T^{(i,j)}\right)$ and $\mu_{R_{\mathrm{max}}}\left(T^{(i,j)}\right)$ from Eq. (1), and $\sigma_{V_{\mathrm{max}}}\left(T^{(i,j)}\right)$ and $\sigma_{R_{\mathrm{max}}}\left(T^{(i,j)}\right)$ from Eq. (2). Set $\mu_{V_{\mathrm{t}}} = 6.02$ m/s and $\sigma_{V_{\mathrm{t}}} = 2.45$m/s.
      - Sample $V_{\mathrm{max}}^{(i,j)}$, $R_{\mathrm{max}}^{(i,j)}$, and $V_{\mathrm{t}}^{(i,j)}$ from the distributions given in Table 3.
      - Sample $A^{(i,j)}, n^{(i,j)}$, and $X_1^{(i,j)}$ using a Nataf's model based on the probability distributions given in Table 3.
      - Calculate $V_{\mathrm{r}}^{(i,j)}$ from Eq. (5).
      - Sample $\beta^{(i,j)}$ from the distribution given in Table 3 and calculate $\alpha^{(i,j)}$.
      - Calculate $V^{(i,j)}$ at the site from Eq. (6).
  - End if

End for

Figure 4

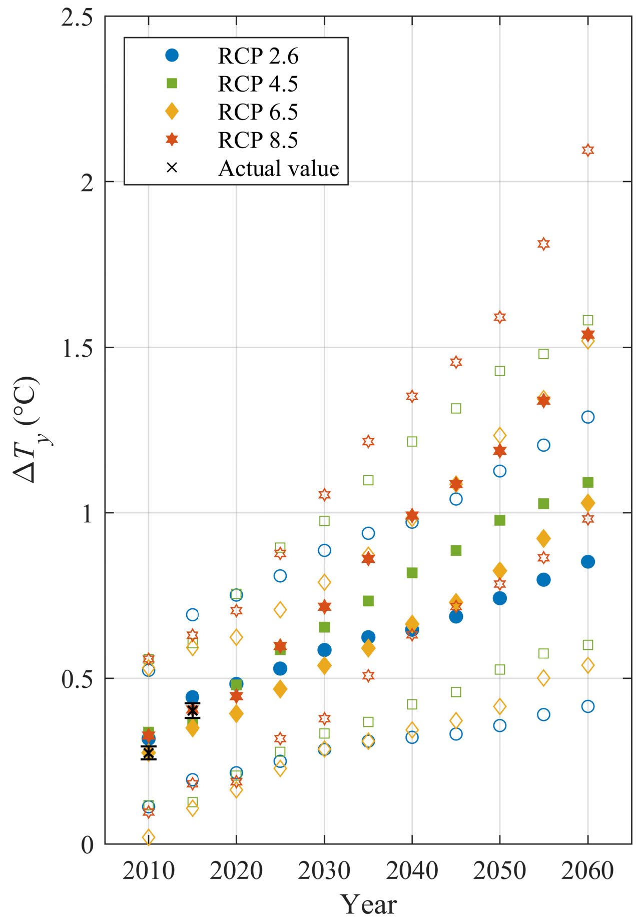

2.5
2
1.5
1
0.5
0
ΔT_y (°C)
2010
2020
2030
2040
2050
2060
Year
RCP 2.6
RCP 4.5
RCP 6.5
RCP 8.5
Actual value

Figure 5

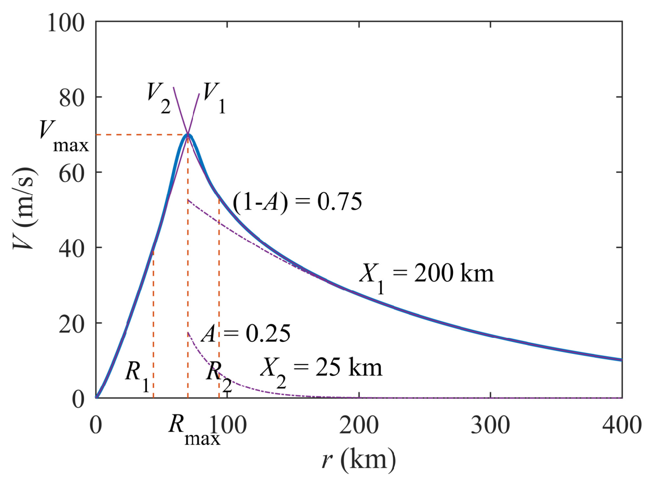

100
80
60
40
20
0
V (m/s)
V_2
V_1
V_max
(1-A) = 0.75
X_1 = 200 km
A = 0.25
R_1
R_2
X_2 = 25 km
0
R_max
100
200
300
400
r (km)

Figure 6

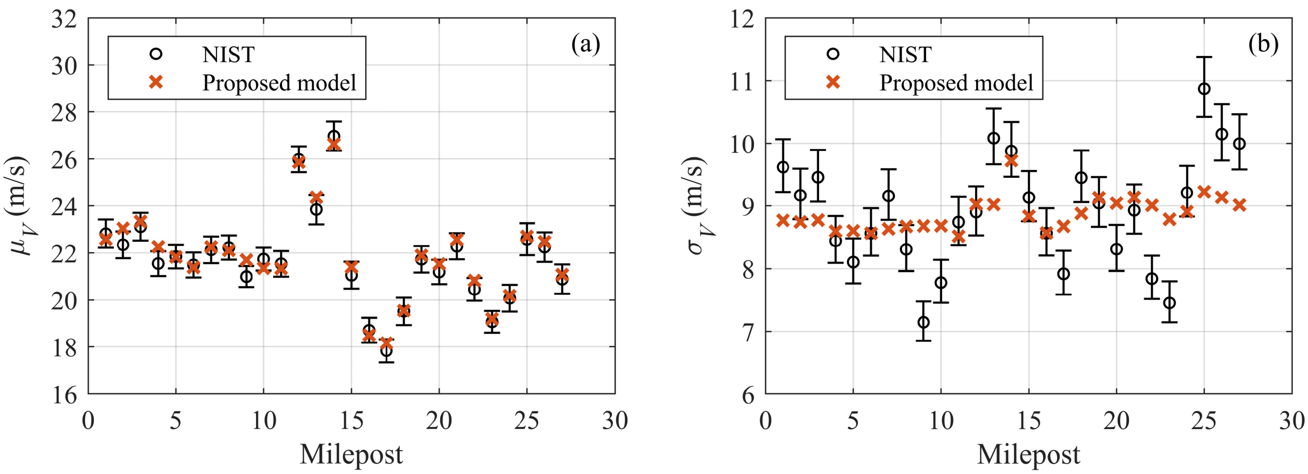

NIST
Proposed model
(a)
μ_V (m/s)
Milepost
32
30
28
26
24
22
20
18
16
0
5
10
15
20
25
30
NIST
Proposed model
(b)
σ_V (m/s)
Milepost
12
11
10
9
8
7
6
0
5
10
15
20
25
30

Figure 7

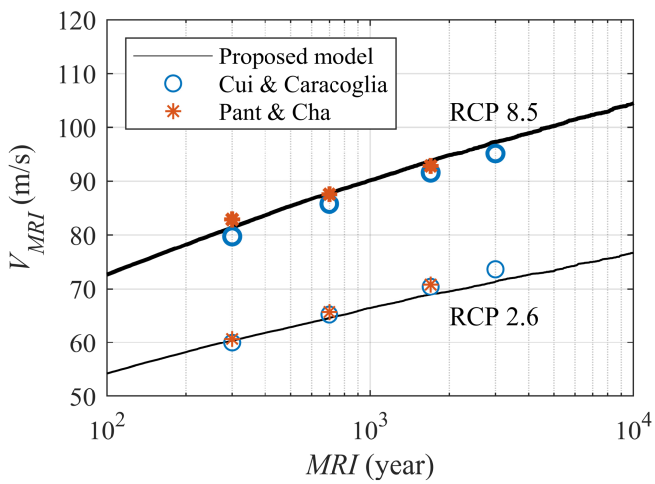

Proposed model
Cui & Caracoglia
Pant & Cha
RCP 8.5
RCP 2.6
V_{MRI} (m/s)
MRI (year)
120
110
100
90
80
70
60
50
10^2
10^3
10^4